

Analysis of a photon number resolving detector based on fluorescence readout of an ion  
Coulomb crystal quantum memory inside an optical cavity

This article has been downloaded from IOPscience. Please scroll down to see the full text article.

2013 New J. Phys. 15 025021

(<http://iopscience.iop.org/1367-2630/15/2/025021>)

View [the table of contents for this issue](#), or go to the [journal homepage](#) for more

Download details:

IP Address: 130.225.29.254

The article was downloaded on 03/05/2013 at 12:58

Please note that [terms and conditions apply](#).

## Analysis of a photon number resolving detector based on fluorescence readout of an ion Coulomb crystal quantum memory inside an optical cavity

Christoph Clausen<sup>1,3</sup>, Nicolas Sangouard<sup>1</sup>  
and Michael Drewsen<sup>2</sup>

<sup>1</sup> Group of Applied Physics, University of Geneva, CH-1211 Geneva 4, Switzerland

<sup>2</sup> QUANTOP, Danish National Research Foundation Center for Quantum Optics, Department of Physics and Astronomy, Aarhus University, DK-8000 Aarhus C, Denmark

E-mail: [christoph.clausen@unige.ch](mailto:christoph.clausen@unige.ch)

*New Journal of Physics* **15** (2013) 025021 (10pp)

Received 10 September 2012

Published 14 February 2013

Online at <http://www.njp.org/>

doi:10.1088/1367-2630/15/2/025021

**Abstract.** The ability to detect single photons with a high efficiency is a crucial requirement for various quantum information applications. By combining the storage process of a quantum memory for photons with fluorescence-based quantum state measurement, it is, in principle, possible to achieve high-efficiency photon counting in large ensembles of atoms. The large number of atoms can, however, pose significant problems in terms of noise stemming from imperfect initial state preparation and off-resonant fluorescence. We identify and analyse a concrete implementation of a photon number resolving detector based on an ion Coulomb crystal inside a moderately high-finesse optical cavity. The cavity enhancement leads to an effective optical depth of 15 for a finesse of 3000 with only about 1500 ions interacting with the light field. We show that these values allow for essentially noiseless detection with an efficiency larger than 93%. Moderate experimental parameters allow for repetition rates of about 3 kHz,

<sup>3</sup> Author to whom any correspondence should be addressed.



Content from this work may be used under the terms of the [Creative Commons Attribution-NonCommercial-ShareAlike 3.0 licence](https://creativecommons.org/licenses/by-nc-sa/3.0/). Any further distribution of this work must maintain attribution to the author(s) and the title of the work, journal citation and DOI.

limited by the time needed for fluorescence collection and re-cooling of the ions between trials. Our analysis may lead to the first implementation of a photon number resolving detector in atomic ensembles.

## Contents

<b>1. Introduction</b>	<b>2</b>
<b>2. Protocol</b>	<b>5</b>
2.1. Initialization . . . . .	5
2.2. Light storage . . . . .	6
2.3. Fluorescence collection . . . . .	7
<b>3. Conclusion</b>	<b>9</b>
<b>Acknowledgments</b>	<b>9</b>
<b>References</b>	<b>10</b>

## 1. Introduction

Photons have repeatedly been proved to be excellent carriers of quantum information [1]. As such they play important roles in experiments that investigate the fundamental aspects of quantum mechanics, as well as in emerging quantum technologies. The final step in many of these scenarios is the detection of photons, making the detection efficiency a central parameter. Additionally, the number of photons in the experiments increases steadily, and as of today entangled states of as many as eight photons have been created [2]. Increasing the photon number even further will be extremely difficult without high-efficiency detectors. At the same time, some of the most fundamental experiments with not more than two photons have equally strong requirements. Loophole-free tests of Bell's inequalities, for example, can ascertain the non-local character of quantum mechanics, provided that the overall detection efficiency is greater than 82.8% [3].<sup>4</sup> Still higher requirements are set by linear optics quantum computing based on realistic single-photon sources, where scalable entanglement-generating gates can only be achieved for a detection efficiency greater than 90% [4]. Additionally, these gates need detectors that can distinguish a single-photon event from events with zero or multiple photons, i.e. a basic form of photon number resolution. The ability to distinguish different numbers of photons is an asset in many other situations. For example, it simplifies the implementation of device-independent quantum key distribution, where the security of the key does not depend on the devices used for its generation [5]. It also opens up new opportunities in fundamental physics, such as the exploration of entanglement between microscopic and macroscopic objects [6].

The high demands set by quantum optics applications have in recent years led to significant developments in single-photon detection technologies. State-of-the-art silicon-based avalanche photo diodes have peak efficiencies of around 70% and low dark count rates, but currently the ability to distinguish photon numbers remains limited [7]. Detectors that reach efficiencies above 90% while at the same time maintaining a low dark count rate are still scarce [8]. Only recently, close to unity efficiency and negligible dark counts have been demonstrated with

<sup>4</sup> It is possible to relax the requirement on the detection efficiency down to  $\eta = 2/3$  by using non-maximally entangled states [3]. However, this requires extreme signal-to-noise ratios.

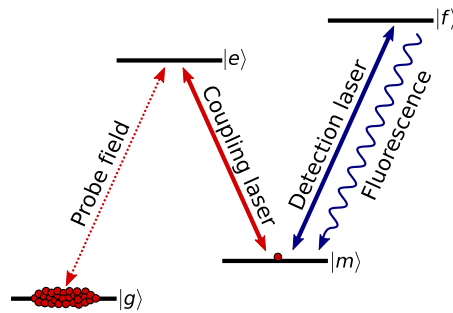


**Figure 1.** Principle of the atom-based photon detector as originally proposed in [10, 11]. First, an ensemble of identical atoms is prepared in their ground state  $|g\rangle$ . Next, photons in the probe field are converted into collective excitations in the metastable state  $|m\rangle$  with the help of a coupling laser. Finally, the number of collective excitations is probed by collecting fluorescence on the closed transition  $|m\rangle \leftrightarrow |f\rangle$ .

transition edge sensors [9]. While these devices also show photon number resolution for small photon numbers, their low operating temperature of 100 mK requires sophisticated cooling technology.

We present a feasibility study of a high-efficiency photon number resolving detector based on a Coulomb crystal of  $^{40}\text{Ca}^+$  ions placed inside an optical cavity. Our scheme is a cavity-based implementation of previous proposals suggesting the use of an ensemble of atoms to convert a single photon into many fluorescence photons, which are then readily detected [10, 11]. The fact that our cavity-based scheme only requires a moderate number of ions removes a series of problems which would have strongly limited the usefulness of possible implementations without a cavity. At the same time, high efficiency can still be reached with a relatively small number of ions and a moderate finesse cavity, making faithful photon counting feasible.

The gist of the original proposals [10, 11] is illustrated by means of the energy level diagram in figure 1. They suggest to combine two key technologies. First, photons in a probe pulse are coherently converted into collective excitations in an atomic ensemble using light storage based on electromagnetically induced transparency (EIT) [12]. Then the number of collective excitations is probed by measuring resonance fluorescence as usually employed in ion trap experiments [13]. The whole procedure works as follows. An ensemble of atoms is initially prepared in a specific ground state  $|g\rangle$ . The light field to be measured is resonant with the transition  $|g\rangle \leftrightarrow |e\rangle$ . It takes the role of the probe field in an EIT scheme, and is coherently mapped onto a collective excitation in the metastable state  $|m\rangle$  by applying a strong coupling laser on the transition  $|m\rangle \leftrightarrow |e\rangle$ . Finally, a detection laser couples  $|m\rangle$  to a fourth state  $|f\rangle$ , which spontaneously decays back to  $|m\rangle$  only. The scheme inherently exhibits photon number resolution since the amount of fluorescence emitted on the transition  $|m\rangle \leftrightarrow |f\rangle$  is directly proportional to the number of photons in the probe field.

The conversion of the photons in the probe field into collective excitations in the atomic ensemble can, in principle, be made arbitrarily efficient by increasing the number of atoms in the ensemble. For a cold gas the required number of atoms is of the order of  $N = 10^6$ . Such a large number of atoms leads to a series of technical problems. The first problem arises during the initialization of the atoms. Since any atom in  $|m\rangle$  will contribute to the fluorescence at

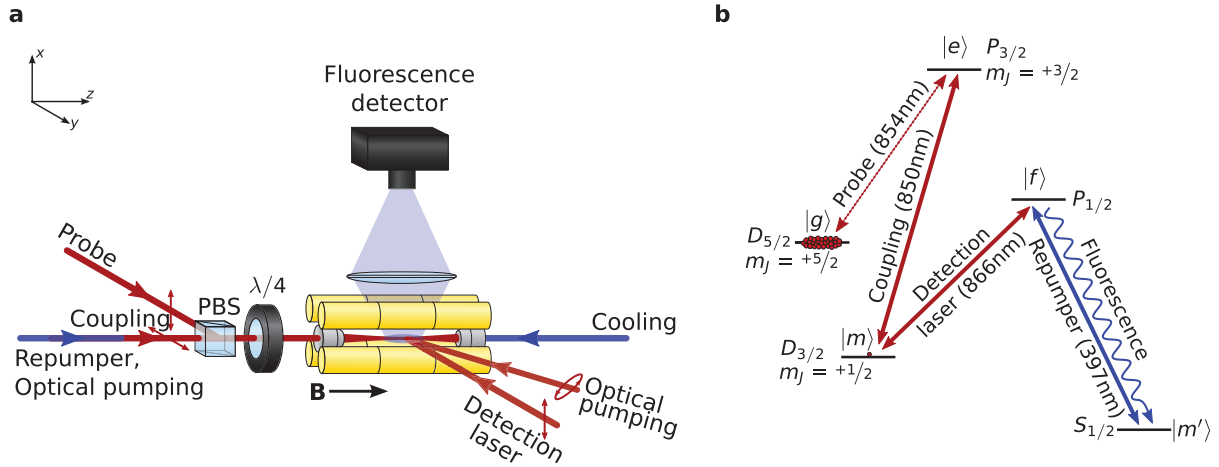


**Figure 2.** Implementation of the photon detector based on a Coulomb crystal of  $^{40}\text{Ca}^+$  ions inside an optical cavity. (a) The laser beams for cooling, optical pumping, as well as the probe and coupling fields travel along the cavity axis in order to avoid Doppler shifts due to rf-induced micromotion [15, 16]. Additional laser beams are used in a second optical pumping step and exciting fluorescence. The fluorescence is collected with a large numerical aperture lens and is directed towards a detector. (b) A diagram showing which energy levels of  $^{40}\text{Ca}^+$  take the roles specified in figure 1.

the detection stage, this state has to be emptied completely, requiring optical pumping with an extremely high efficiency. For alkali atoms, considered in the original proposals, the states  $|g\rangle$  and  $|m\rangle$  would typically belong to the two hyperfine manifolds of the  $S_{1/2}$  ground state, separated in energy by a hyperfine splitting  $\Delta_{\text{HFS}}$  of the order of a few gigahertz. The state  $|f\rangle$  is part of the  $P_{3/2}$  manifold with a line width  $\Gamma \approx 10$  MHz. The probability of unwanted off-resonant excitation of an atom from  $|g\rangle$  during the detection stage is of the order of  $\Gamma^2/\Delta_{\text{HFS}}^2 \approx 10^{-6}$ . For 1 million atoms this noise is comparable with the signal from a few-photon probe field. Finally, the collection of a sufficient amount of fluorescence can be impeded by a premature loss of the atoms from the trap caused by heating and light-assisted collisions [14].

A concrete system that significantly reduces or avoids the problems mentioned above is shown in figure 2. It consists of an ion Coulomb crystal [17, 18] with  $N \approx 1500$   $\text{Ca}^+$  ions interacting with the field of an optical cavity with a moderately high finesse of  $\mathcal{F} \approx 3000$ . In the ions, the metastable states  $D_{5/2}$  and  $D_{3/2}$  (lifetimes  $\sim 1.15$  s) take the roles of  $|g\rangle$  and  $|m\rangle$ , respectively, while  $P_{3/2}$  is  $|e\rangle$  and  $P_{1/2}$  is  $|f\rangle$ . Since ions in the  $P_{1/2}$  ( $|f\rangle$ ) state can spontaneously decay to  $S_{1/2}$  ( $|m'\rangle$ ), a repumper is needed to address the  $|f\rangle \leftrightarrow |m'\rangle$  transition. The fluorescence rate on this transition is, in fact, more than ten times as high as that on the  $|f\rangle \leftrightarrow |m\rangle$  transition and hence is most optimal for the final fluorescence detection.

The essential ingredients of the proposed photon detector have already been applied in recent experiments, demonstrating strong collective coupling [19] and cavity EIT [20]. While the experiments reported in [19, 20] were carried out between sub-states of the  $D_{3/2}$  level only, very efficient ( $> 90\%$ ) population transfer between  $D_{3/2}$  and  $D_{5/2}$  states had been obtained in earlier experiments using stimulated Raman adiabatic passage (STIRAP) [21].

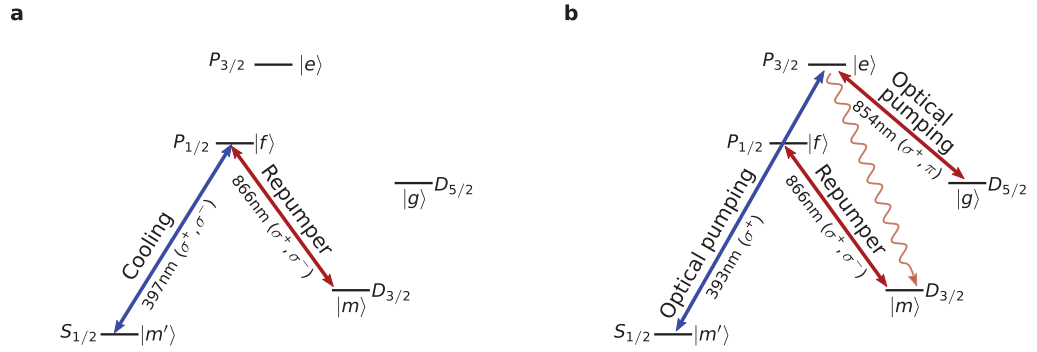


**Figure 3.** Energy levels and relevant transitions for the initialization of the photon detector in  $^{40}\text{Ca}^+$ . (a) The ions are laser cooled by driving the  $S_{1/2} \leftrightarrow P_{1/2}$  transition at 397 nm and repumping on the  $D_{3/2} \leftrightarrow P_{1/2}$  transition at 866 nm. (b) Optical pumping to the  $m_J = +5/2$  Zeeman sub-state of the  $D_{5/2}$  level is accomplished by two optical pumping beams on the  $S_{1/2} \leftrightarrow P_{3/2}$  (393 nm) and  $D_{5/2} \leftrightarrow P_{3/2}$  (854 nm) transitions. The repumper takes care of atoms that spontaneously decay from  $P_{3/2}$  to  $D_{3/2}$ .

## 2. Protocol

In the following, the individual steps of the photon detection protocol will be discussed in detail. Every step of the protocol determines one of the characteristics of the detector: the successful initialization significantly reduces the probability of dark counts, the probability of successful light storage is equal to the overall efficiency of the detector, and the time required for fluorescence collection limits the repetition rate of the detector.

### 2.1. Initialization

The goal of the initialization is preparation of a cold Coulomb crystal with the ions in the state  $|g\rangle = |D_{5/2}, m_J = +5/2\rangle$ . The preparation consists of several steps similar to the preparation described in [19]. A magnetic field of a few Gauss along the cavity axis defines the quantization axis, and laser cooling is achieved by applying two counter-propagating light beams along the cavity axis. The light is resonant with the  $S_{1/2} \leftrightarrow P_{1/2}$  transition at 397 nm, and the beams are left- and right-hand circularly polarized, respectively (see figure 3). Atoms that fall into the  $D_{3/2}$  state are repumped by a laser at 866 nm applied from the side with its polarization orthogonal to the cavity axis, equivalent to left- and right-hand circularly polarized with respect to the quantization axis. Once the ions are sufficiently cold, the cooling laser is turned off. Two additional lasers pump the ions to the  $m_J = +5/2$  Zeeman sub-level of the  $D_{5/2}$  state. The first of these lasers drives the  $\sigma^+$ -transitions from  $S_{1/2}$  to  $P_{3/2}$ . The second laser is resonant with the  $D_{5/2} \leftrightarrow P_{3/2}$  transition, and its propagation direction and polarization are chosen such that  $\sigma^+$  and  $\pi$  transitions are addressed simultaneously. Atoms that spontaneously decay from  $P_{3/2}$  to  $D_{3/2}$  are reintroduced into the optical pumping process by the laser cooling repumper. The typical duration of the cooling and pumping procedure is 25  $\mu\text{s}$  [22].

Efficient optical pumping is very important for high-fidelity measurements of the photon number in the probe field. Ions that are not in the state  $|g\rangle$  after the initialization may offset

the fluorescence in the final step of the detector protocol, leading to an overestimation of the photon number. Herskind *et al* [19] state an optical pumping efficiency to the  $D_{3/2}$  level with  $m_J = +3/2$  of 97%. Optical pumping into the  $m_J = +5/2$  sub-state of the  $D_{5/2}$  state is expected to have a similar efficiency. The efficiency is limited by imperfect polarization of the pumping light, leading to a distribution of the remaining ions over the other  $D_{5/2}$  sub-states. The spontaneous decay rate into  $D_{3/2}$  of only  $2\pi \times 0.18$  MHz is very weak compared to the pumping and repumping fields, so only a tiny fraction of the ions will end up in  $S_{1/2}$  or  $D_{3/2}$ . The number of these ions can be estimated by monitoring the ultraviolet fluorescence during the optical pumping, and the result subtracted from the photon number measurement at the end of the protocol. Alternatively, one can extend the dead time of the detector by a variable amount and let optical pumping proceed until the moment when the monitored fluorescence ceases. This signals that the relevant energy levels are empty, and the detector is ready to receive the probe pulse. We note that the larger the total number of ions, the more difficult it is to transfer *all* ions to  $D_{5/2}$ , making a moderate number of ions the preferred choice.

## 2.2. Light storage

In the second step of the detector protocol, the photons in the probe pulse are converted into collective excitations in the metastable state  $|m\rangle$ . The procedure is the same as the absorption of photons into a quantum memory for light, based on an ensemble placed inside an optical cavity [23]. We consider a storage scheme based on EIT, where the probe pulse is resonant with the  $\sigma^-$  transition  $|D_{5/2}, m_J = +5/2\rangle \leftrightarrow |P_{3/2}, m_J = +3/2\rangle$ . At the same time a strong coupling field is acting on the transition  $|P_{3/2}, m_J = +3/2\rangle \leftrightarrow |D_{3/2}, m_J = +1/2\rangle$  (see also figure 2). The strength of the coupling field determines the width of the EIT window and the group velocity of the probe pulse. One can coherently convert the quantum state of the probe pulse into a collective excitation by reducing the group velocity to zero, that is, by adiabatically turning off the coupling field.

The most essential parameter of such memories is the cooperativity  $C = g^2 N / \kappa \gamma$ , where  $g$  is the coupling rate between a single ion and a cavity photon,  $N$  is the *effective*<sup>5</sup> number of ions interacting with the mode of the cavity [19],  $\kappa$  is the cavity decay rate and  $\gamma$  is the rate of decoherence on the transition  $|g\rangle \leftrightarrow |e\rangle$  in the protocol. The cooperativity determines the maximally obtainable photon conversion efficiency  $\eta = C / (1 + C)$  [24]. In principle, probe pulses of any temporal shape can be stored with optimal efficiency by adapting the shape of the coupling field. However, the adiabatic conversion of photons into collective excitations requires that the temporal length  $T$  of the photonic probe pulse is much larger than  $1/C\gamma$  [24, 25]. Optimal storage and retrieval with an efficiency of  $\eta^2 \simeq 45\%$  has been demonstrated using EIT in rubidium vapour [26] without cavity. Using a low-finesse cavity, a retrieval efficiency of 73% was recently obtained with cold atoms [27] using a Raman scheme that has the same adiabaticity conditions as EIT.

The efficiency of the light storage determines the overall detection efficiency, as long as saturation effects are avoided by ensuring that the number of photons in the probe pulse is much smaller than the number of ions. The experimental parameters obtained in [19] on the transition  $|D_{3/2}, m_J = +3/2\rangle \leftrightarrow |P_{1/2}, m_J = +1/2\rangle$  are ( $g = 2\pi \times 0.53$  MHz,  $N \simeq 1500$ ,  $\kappa = 2\pi \times 2.15$  MHz,  $\gamma = 2\pi \times 11.9$  MHz), giving a maximum cooperativity<sup>6</sup> of  $C \simeq 16$ .

<sup>5</sup> The total number of ions may be a factor of 10 larger.

<sup>6</sup> Please note that the definition of the cooperativity in [19] differs from the one used here by a factor of 2.



For the transition  $|D_{5/2}, m_J = +5/2\rangle \leftrightarrow |P_{3/2}, m_J = +3/2\rangle$  used in our protocol, the theoretical values for  $g$  and  $\gamma$  are slightly higher. Hence, a cooperativity of  $C \simeq 15$  should be straightforward to obtain, which gives a detection efficiency above 93%.

The duration of the storage process is essentially given by the duration of the probe pulse. We find that  $C\gamma \approx 10^9 \text{ s}^{-1}$ , allowing, in principle, for the optimal storage of Fourier-limited pulses of duration down to about  $T \simeq 50/C\gamma = 50 \text{ ns}$  [24], but even a more conservative value of  $1 \mu\text{s}$  is negligible compared to the duration of the entire protocol.

To avoid unwanted Doppler effects related to rf-induced micromotion (see references in the caption of figure 2), the coupling field has to co-propagate with the probe field inside the cavity, as indicated in figure 2. In this case the geometrical constraints on the spatial profile of the coupling field reduce the optimal storage efficiency by an amount that depends on the radial extension of the Coulomb crystal. However, this reduction can be rendered negligible by carefully choosing the size of the crystal, adjusting the strength of the coupling field or constraining the radius by the addition of a second calcium isotope [25].

### 2.3. Fluorescence collection

In the last step of the protocol, the number of ions transferred to the  $D_{3/2}$  state is measured by fluorescence collection. Fluorescence collection is routinely applied in trapped-ion-based quantum computing, and a single-ion state-discrimination with an error probability below  $10^{-4}$  has been reported [28]. The fluorescence is induced by the same lasers that were used during the cooling stage (figure 3(a)). Ions in one of the  $D_{3/2}$  will emit fluorescence on the  $S_{1/2} \leftrightarrow P_{1/2}$  transition. The amount of fluorescence is proportional to the number of ions undergoing the optical cycling. For unity absorption efficiency and the ideal initialization of the detector, this number is equal to the number of photons originally present in the probe pulse. Since the detection laser is 12 nm detuned from the  $D_{5/2} \leftrightarrow P_{3/2}$  transition, the ions that remained in  $D_{5/2}$  are not affected at all. However, because the lifetime of the D-states is finite ( $\tau_D = 1.15 \text{ s}$ ), ions in  $D_{5/2}$  can still enter the fluorescence cycle by spontaneously decaying into  $S_{1/2}$ .

We now analyse the process of fluorescence collection in a more quantitative way. The Poissonian statistics of the detected fluorescence photons is taken into account, and the fidelity of the photon number estimation discussed. Let us start by considering  $\eta = 1$  and  $N_{\text{in}}$  photons in the probe pulse. Assuming that all the involved optical transitions are saturated, every ion spends about 1/4 of its time in  $P_{1/2}$ , from where it spontaneously decays into  $S_{1/2}$  at a rate of  $\gamma_{\text{PS}} = 2\pi \times 20.7 \text{ MHz}$ . Letting  $\Theta$  denote the amount of solid angle covered by the collection system and  $\eta_D$  the overall detection efficiency at the relevant wavelength of 397 nm, the photon detection rate per ion is given by  $R = \gamma_{\text{PS}}\Theta\eta_D/16\pi$ . A typical detector has  $\eta_D = 0.4$ , and a lens with 4 cm diameter at a working distance of 7 cm can cover about  $\Theta/4\pi = 2\%$  of the full solid angle and still image the whole crystal, albeit with some distortion. These parameters give  $R = 260 \text{ kHz}$ . The total number of photons collected after a time  $t$  will follow a Poissonian distribution with the mean

$$\mu_{\text{in}}(t) = N_{\text{in}} R t. \quad (1)$$

At any intermediate time  $t'$ , the mean number of ions having decayed from  $D_{5/2}$  is  $N(1 - e^{-t'/\tau_D})$ , neglecting the time passed since the initial state preparation. After a time  $t$ , the mean number of collected fluorescence photons from these ions is

$$\mu_{\text{decay}}(t) = \int_0^t N(1 - e^{-t'/\tau_D}) R dt' = N R \tau_D [(e^{-t/\tau_D} - 1) + t/\tau_D]. \quad (2)$$



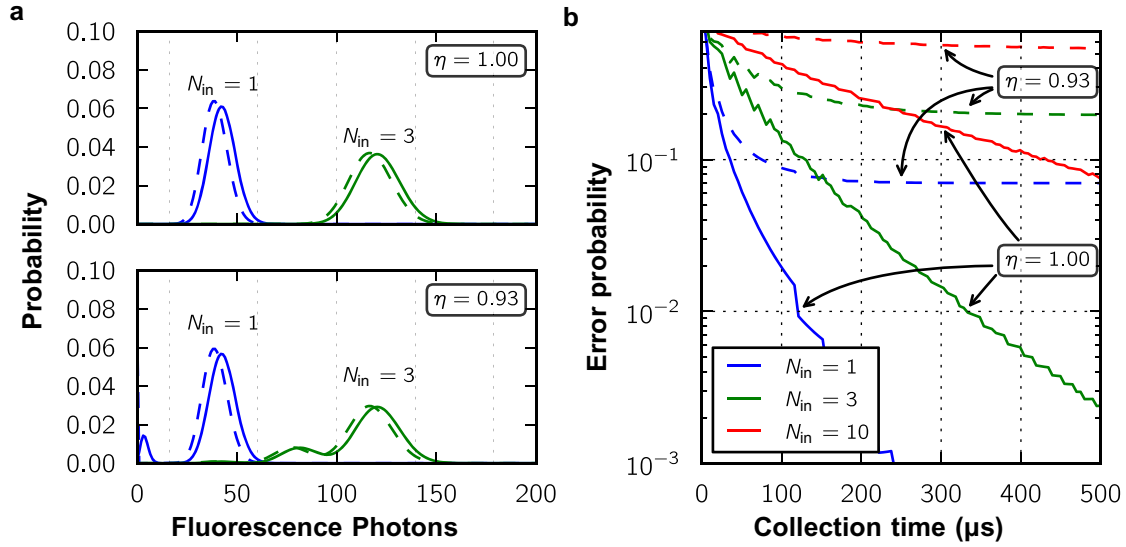


**Figure 4.** Estimation of the input photon number and the associated error probability. (a) Fluorescence photon number distribution for  $N_{in} = 1$  and 3 input photons for a collection time of  $150 \mu s$ . The upper plot shows the case of the ideal conversion efficiency. Dashed lines are without the contribution from the spontaneous decay of ions from the  $D_{5/2}$  state. Vertical dashed lines indicate the thresholds for photon number estimation. In the lower plot the finite conversion efficiency ( $\eta = 0.93$ ) leads to the possibility of estimating a photon number lower than  $N_{in}$ . (b) Probability of estimating a photon number different from  $N_{in}$ , for  $N_{in} = 1, 3$  or  $10$ . The error probability decreases with collection time, but has a lower limit for finite conversion efficiency.

The probability of detecting  $N_{fl}$  fluorescence photons after a time  $t$  is then given by

$$p_{N_{fl}}(t) = \sum_{n=0}^{N_{fl}} \text{Po}[n; \mu_{in}(t)] \text{Po}[N_{fl} - n; \mu_{decay}(t)] = \text{Po}[N_{fl}; \mu_{in}(t) + \mu_{decay}(t)], \quad (3)$$

where  $\text{Po}[n; \mu]$  denotes the Poisson distribution with the mean  $\mu$ . So, the spontaneously decaying ions shift the amount of fluorescence to slightly higher values without changing the shape of the distribution. This is illustrated in figure 4(a) for  $N = 1500$  ions.

The time required for fluorescence collection depends on the amount of confidence in the estimated input photon number that one wants to obtain. We consider a simple strategy, where the input is estimated as  $N_{in}$  photons if the amount of fluorescence is larger than a threshold that corresponds to the point where the Poisson distributions for  $N_{in}$  and  $N_{in} - 1$  input photons cross, see figure 4(a). As a measure of the fidelity, we will consider the probability that  $N_{in}$  input photons lead to an estimate that is different from  $N_{in}$ . This error probability is plotted as a function of the collection time in figure 4(b) for  $N_{in} = 1, 3$  or  $10$  photons. The larger the  $N_{in}$ , the more the fluorescence needed to reduce the error below a certain level. For the parameters considered here and an error probability below 10%, one can distinguish up to three photons after  $t \simeq 130 \mu s$  and ten photons after  $t \simeq 430 \mu s$ .

In the case where  $\eta < 1$ , the number of ions transferred to  $|m\rangle$  follows a binomial distribution, that is, not all photons are necessarily converted into collective excitations. In fact,

the probability that *all* input photons are converted is  $\eta^{N_{\text{in}}}$ , which sets a lower bound on the error probability of  $p_{\text{err}}^{\text{min}} = 1 - \eta^{N_{\text{in}}}$ . We note that this lower bound is valid for *any* photon number resolving detector with non-unity efficiency. For our parameters, the bound is obtained after  $t \simeq 180 \mu\text{s}$  for  $N_{\text{in}} = 1$  and  $t \simeq 250 \mu\text{s}$  for  $N_{\text{in}} = 3$ .

After the fluorescence detection, the ions will have to undergo a brief period of laser cooling before reinitialization back into  $D_{5/2}$ . Based on previous experiments [19, 20], this procedure is expected to take less than  $100 \mu\text{s}$ .

To calculate the repetition rate, we add up the durations of the individual steps of the protocol, neglecting the short duration of the light storage. Using the numbers stated in the previous sections, we obtain  $T_{\text{total}} \simeq (25 + 200 + 100) \mu\text{s}$ , giving a repetition rate of about 3 kHz.

### 3. Conclusion

In summary, we have presented a concrete implementation of an atomic-ensemble-based photon number resolving detector based on a Coulomb crystal of  $^{40}\text{Ca}^+$  ions inside an optical cavity. For the currently available system, a detection efficiency of  $\eta \approx 93\%$  is already feasible. The efficiency can be improved by increasing the cooperativity, e.g. by applying a cavity with a higher finesse, a larger Coulomb crystal and/or spatially controlling the ions positions with respect to the anti-nodes of the standing-wave light field [29, 30]. A detection efficiency of better than 98% is thus within reach. Different photon numbers can be distinguished as long as the number of photons is much lower than the number of ions. For 1500 ions, photon number resolution can probably be maintained up to a few tens of photons. However, for more than  $\sim 10$  input photons the non-unity detection efficiency and the Poissonian counting statistics of fluorescence will limit the achievable fidelity. Furthermore, it should be possible to reduce the dark counts to a negligible level, provided that the quality of the initialization can be assured. On the downside, the detector can be considered as rather slow in terms of repetition rate. Currently, the repetition rate would be limited to about 3 kHz, caused by the rather long fluorescence detection and cooling steps. Improvements of the experimental setup could probably push this to about one measurement every  $50 \mu\text{s}$ . This would correspond to the time it takes for a signal to travel through 10 km of optical fibre, and should hence be sufficient for, e.g., the next generation of long-distance quantum communication experiments [31]. The bandwidth of the photons in the probe pulse is limited by the adiabaticity condition  $T \gg 1/C\gamma$  for the light storage. For our proposed implementation using  $^{40}\text{Ca}$ , this translates into a minimum Fourier-limited duration of the input pulse of about 50 ns. The improvements of the cooperativity discussed above can probably gain a factor of 4–5. However, many tasks in optical quantum information processing also necessitate quantum memories, whose bandwidth is equally limited. In fact, the kind of photon detector presented here is a quantum memory without retrieval, and it is imaginable that other kinds of quantum memories can be used in a similar way, extending the range of applications for quantum memories significantly.

### Acknowledgments

We are grateful for discussions with Mikael Afzelius, Aurelien Dantan, Nicolas Gisin, Philippe Goldner, Jean-Louis Le Gouët, Rob Thew and Hugo Zbinden. CC and NS acknowledge financial support from the ERC Advanced Grant QORE and from the Swiss NCCR ‘Quantum Science and Technology’. MD acknowledges financial support from the Carlsberg Foundation

and the EU via the FP7 projects ‘Physics of Ion Coulomb Crystals’ and ‘Circuit and Cavity Electrodynamics’.

## References

- [1] Gisin N and Thew R 2007 *Nature Photon.* **1** 165
- [2] Yao X-C, Wang T-X, Xu P, Lu H, Pan G-S, Bao X-H, Peng C-Z, Lu C-Y, Chen Y-A and Pan J-W 2012 *Nature Photon.* **6** 225
- [3] Eberhard P H 1993 *Phys. Rev. A* **47** R747
- [4] Jennewein T, Barbieri M and White A G 2011 *J. Mod. Opt.* **58** 276
- [5] Curty M and Moroder T 2011 *Phys. Rev. A* **84** 010304
- [6] Raeisi S, Sekatski P and Simon C 2011 *Phys. Rev. Lett.* **107** 250401
- [7] Thomas O, Yuan Z L, Dynes J F, Sharpe A W and Shields A J 2010 *Appl. Phys. Lett.* **97** 031102
- [8] Hadfield R H 2009 *Nature Photon.* **3** 696
- [9] Lita A E, Miller A J and Nam S W 2008 *Opt. Express* **16** 3032
- [10] James D F V and Kwiat P G 2002 *Phys. Rev. Lett.* **89** 183601
- [11] Imamoğlu A 2002 *Phys. Rev. Lett.* **89** 163602
- [12] Fleischhauer M and Lukin M D 2000 *Phys. Rev. Lett.* **84** 5094
- [13] Rowe M A, Kielpinski D, Meyer V, Sackett C A, Itano W M, Monroe C and Wineland D J 2001 *Nature* **409** 791
- [14] DePue M T, McCormick C, Winoto S L, Oliver S and Weiss D S 1999 *Phys. Rev. Lett.* **82** 2262
- [15] Schiffer J P, Drewsen M, Hangst J S and Hornekær L 2000 *Proc. Natl Acad. Sci. USA* **97** 10697
- [16] Landa H, Drewsen M, Reznik B and Retzker A 2012 *New J. Phys.* **14** 093023
- [17] Wineland D J, Bergquist J C, Itano W M, Bollinger J J and Manney C H 1987 *Phys. Rev. Lett.* **59** 2935
- [18] Diedrich F, Peik E, Chen J M, Quint W and Walther H 1987 *Phys. Rev. Lett.* **59** 2931
- [19] Herskind P F, Dantan A, Marler J P, Albert M and Drewsen M 2009 *Nature Phys.* **5** 494
- [20] Albert M, Dantan A and Drewsen M 2011 *Nature Photon.* **5** 633
- [21] Sørensen J L, Møller D, Iversen T, Thomsen J B, Jensen F, Staunum P, Voigt D and Drewsen M 2006 *New J. Phys.* **8** 261
- [22] Albert M 2010 *PhD Thesis* Aarhus University, Denmark
- [23] Lukin M D, Yelin S F and Fleischhauer M 2000 *Phys. Rev. Lett.* **84** 4232
- [24] Gorshkov A V, André A, Lukin M D and Sørensen A S 2007 *Phys. Rev. A* **76** 033804
- [25] Zangenberg K R, Dantan A and Drewsen M 2012 *J. Phys. B: At. Mol. Opt. Phys.* **45** 124011
- [26] Phillips N B, Gorshkov A V and Novikova I 2008 *Phys. Rev. A* **78** 023801
- [27] Bao X-H, Reingruber A, Dietrich P, Rui J, Duck A, Strassel T, Li L, Liu N-L, Zhao B and Pan J-W 2012 *Nature Phys.* **8** 517
- [28] Myerson A H, Szwer D J, Webster S C, Allcock D T C, Curtis M J, Imreh G, Sherman J A, Stacey D N, Steane A M and Lucas D M 2008 *Phys. Rev. Lett.* **100** 200502
- [29] Linnet R B, Leroux I D, Marcianti M, Dantan A and Drewsen M 2012 arXiv:1208.4005
- [30] Enderlein M, Huber T, Schneider C and Schaetz T 2012 arXiv:1208.3329
- [31] Sangouard N, Simon C, de Riedmatten H and Gisin N 2011 *Rev. Mod. Phys.* **83** 33